Orbital angular momentum exchange in post-collision interaction

J. Phys. B: At. Mol. Phys. 18 (1985) 999-1009. Printed in Great Britain

Orbital angular momentum exchange in post-collision interaction

P J M van der Burgt, J van Eck and H G M Heideman

Fysisch Laboratorium der Rijksuniversiteit Utrecht, Princetonplein 5, 3584 CC Utrecht, The Netherlands

Received 23 July 1984, in final form 22 October 1984

Abstract. We have measured the angular distribution of electrons ejected by the $He^{**}(2s^2)^1S$ autoionising state after its electron impact excitation via the $He^-(2s2p^2)^2D$ resonance. Taking into account interference with electrons from the direct ionisation of helium, analysis of this angular distribution provides evidence for angular momentum exchange between ejected and scattered electrons during the post-collision interaction.

1. Introduction

When an autoionising state is excited near its threshold by electron impact the scattered electron is still close to the atom when the latter decays by ejecting an electron. After the autoionisation the ejected and the scattered electron may exchange energy and angular momentum in the Coulomb field of the residual ion, the ejected electron acquiring a higher and the scattered electron a lower energy. The energy exchange may even be large enough for the scattered electron to be captured into a singly excited state of the neutral atom. This so called post-collision interaction (PCI), which also plays a role in several other atomic collision processes, has been reviewed by Read (1975), Niehaus (1977) and Heideman (1980).

Numerous studies have been published on the effects of PCI resulting from the exchange of energy between the scattered and the ejected electron. However, little is known about the exchange of orbital angular momentum during PCI between the two electrons. Some experimental evidence for angular momentum exchange when PCI causes the scattered electron to be captured into a singly excited helium state was presented by Heideman (1980). Observation of the decay of the $He^-(2s2p^2)^2D$ resonance to the $He^{**}(2s^2)^1S$ autoionising state in ejected electron spectra by van de Water and Heideman (1981) also provided evidence for angular momentum exchange. Niehaus and Zwakhals (1983) showed that angular momentum exchange during PCI between a slow photoelectron and a fast Auger electron may lead to observable structure in the PCI broadened Auger line.

Two quantum mechanical models for PCI have been formulated. The shake-down model (Read 1977) is based on the idea that the scattered electron experiences an instantaneous change of charge of the autoionising atom. The semiclassical model formulated by Morgenstern *et al* (1977) is equivalent to the shake-down model as was shown by van de Water and Heideman (1980). According to the shake-down model the transition probability is proportional to an overlap integral of the intial- and

0022-3700/85/050999+11$02.25

final-state wavefunctions of the scattered electron. Therefore angular momentum exchanges are excluded in this model. An optical potential description of PCI effects in the excitation of singly excited states was formulated by van de Water *et al* (1981). Calculations based on this model showed that angular momentum exchanges may be significant in some cases.

In order to find further evidence for angular momentum exchange during PCI we have studied the angular distribution of ejected electrons from the $He^{**}(2s^2)^1S$ state after its excitation via the $He^-(2s2p^2)^2D$ resonance. Since the $He^{**}(2s^2)^1S$ state decays to the ground state $He^+(1s)$ of the helium ion, the initial angular momentum of the ejected electron is fixed at $l_{ej}=0$. Angular momentum exchange during PCI results in $l_{ej}\neq 0$ and may therefore lead to a deviation from isotropy of the angular distribution of ejected electrons. However, measurement of an angular distribution is greatly complicated because the ejected electrons may interfere with electrons from the direct ionisation of helium.

A detailed study of the decay of the $He^-(2s2p^2)^2D$ resonance to the $He^{**}(2s^2)^1S$ autoionising state has already been published by van de Water and Heideman (1981). In their analysis of the resonant excitation they assumed that the main contribution to the resonance structure in the yield of ejected electrons comes from interference with the direct ionisation of helium. In our analysis we do not make this assumption. In § 2 we shall show that the occurrence of interference is closely linked with the question whether or not the scattered electron exchanges angular momentum with the ejected electron. In § 4 we shall present measurements of the yield of ejected electrons as a function of the ejection angle and discuss angular momentum exchange during PCI.

2. Excitation and decay of the autoionising state

Observation of PCI in ejected electron spectra is complicated by the fact that we cannot distinguish between ejected electrons and electrons from the direct ionisation of helium. Due to interference with the direct ionisation channel we do not observe a PCI broadened and shifted peak in the ejected electron spectra but a rather complicated oscillatory structure (see e.g. Baxter *et al* 1979). It is the purpose of this section to give a qualitative analysis of the various interferences which play a role in the resonant excitation and decay of the $He^{**}(2s^2)^1S$ autoionising state.

2.1. Interference effects in the excitation and decay of the autoionising state

The following reaction schemes play a role in the excitation and decay of the $He^{**}(2s^2)^1S$ autoionising state:

$$\begin{array}{lllll}
e+He & \longrightarrow & He^{**}(2s^2)^1S+e_{sc} & \longrightarrow & He^+ + e_{sc} + e_{ej} \\
e+He & \longrightarrow He^-(2s2p^2)^2D \longrightarrow & He^{**}(2s^2)^1S+e_{sc} & \longrightarrow & He^+ + e_{sc} + e_{ej} \\
e+He & \longrightarrow & & & He^+ + e_1 + e_2 \\
(E_i) & & & & (IP)\ (E_{sc})\ (E_{ej}).
\end{array}$$

We ignore decay of the resonance into the direct ionisation channel. The measurements will show that the resonance predominantly decays to the lower lying autoionising states.

After excitation of the autoionising state the scattered electron may leave the atom in several partial waves of different angular momenta: $l_{sc} = 0, 1, 2, \ldots$. The contribution of a particular partial wave to the total excitation cross section in general changes not very much over a small incident energy range. However, the $He^-(2s2p^2)^2D$ resonance causes a rapid variation of the $l_{sc} = 2$ partial wave around 58.3 eV. Due to interference between direct excitation and resonant excitation the probability for excitation and scattering in a $l_{sc} = 2$ wave will have the shape of a Beutler-Fano resonance profile.

If there were no post-collision interaction we would be able to measure this resonance profile by detecting the number of ejected electrons as a function of the incident electron energy. In such a measurement a total excitation cross section is measured because the scattered electrons are not detected. Therefore without PCI the shape of the resonance profile—that is, peak height to dip depth ratio—is independent of the angle at which the ejected electron is detected.

Now consider post-collision interaction. As PCI profiles are interference structures the cross section for production of ejected electrons may be written as:

$$d\sigma/d\Omega = |B|^2 + |A + aq \exp(i\chi)|^2 \tag{2.1}$$

where a is the amplitude for excitation of the autoionising state and $q \exp(i\chi)$ refers to the decay of the autoionising state and subsequent PCI, with the ejected electron eventually moving in a solid angle element $d\Omega$. χ is the relative phase between q and the interfering part A of the direct ionisation cross section. B is the non-interfering part. It is important to note that the variations in the amplitude $q \exp(i\chi)$ are slow compared with the variations in a when the incident electron energy is swept across the resonance. This is clearly seen in the measurements of Baxter *et al* (1979). The effective excitation functions of the $He^{**}(2s2p)^3P$ state measured by them show significant changes over an incident energy range of the order of 1 eV, whereas the $He^-(2s2p^2)^2D$ resonance has a width of 0.05 eV (see Hicks *et al* 1974). Therefore the variations caused by the resonance in the amplitude a for excitation of the $He^{**}(2s^2)^1S$ autoionising state will not be disturbed by the variations with incident energy in the PCI amplitude $q \exp(i\chi)$. Therefore also in the case of PCI we will be able to measure the shape of the resonance profile by detecting ejected electrons as a function of the incident energy and we expect that the shape is to a good approximation independent of the chosen ejected electron energy.

On the other hand the measurements of Baxter *et al* (1979) show rapid changes of the PCI amplitude $q \exp(i\chi)$ as a function of the ejected electron energy. These rapid changes give rise to the familiar PCI line profiles measured when keeping the incident electron energy fixed. As a consequence the size of the resonance will depend strongly on the ejected electron energy at which the incident energy is scanned.

Summarising, we are dealing with two different interference effects.

(i) Interference between direct and resonant excitation of the $He^{**}(2s^2)^1S$ autoionising state. This interference results in a narrow Beutler-Fano resonance profile in the yield of ejected electrons when the incident energy is scanned. The shape of the measured resonance is expected to be independent of the ejection angle and energy of the ejected electrons but the size is expected to depend strongly on the ejected electron energy.

(ii) Interference between ejected electrons from autoionisation and from direct ionisation. The interference manifests itself as rapid changes in the ejected electron yield as a function of ejected electron energy. As a function of the incident energy (at fixed ejected energies) it gives rise to much slower variations.

2.2. Angular momentum exchange following autoionisation

We want to consider in further detail the interference between ejected electrons from autoionisation and from direct ionisation when the autoionising state is excited via the resonance. When measuring ejected electron spectra we do not detect the scattered electron and thus integrate over all angle variables of the scattered electron. Van de Water and Heideman (1981) have argued that such an integration causes the interference term to vanish unless the slow scattered electrons in the autoionisation channel and the ionisation channel have the same angular momentum. After resonant excitation the scattered electron recedes with an angular momentum $l_{sc} = 2$. As the scattered electron in the direct ionisation channel has a very low energy it most probably has an angular momentum $l_i = 0$†. Unless there is an angular momentum exchange during post-collision interaction resulting in $l_{sc} = l_i$, the interference term will vanish. Van de Water and Heideman (1981) have argued that the major contribution to the structure comes from the interference term assuming that the amplitude for resonant excitation is much smaller than the interfering part of the amplitude for direct ionisation. We do not need to make this assumption. Suppose there would be no angular momentum exchange during PCI. In that case the slow scattered electron will keep an angular momentum $l_{sc} = 2$ after resonant excitation and the interference term with the direct ionisation channel will vanish. As the angular momenta of the autoionising state and the He^+ ion are both 0, the ejected electron has $l_{ej} = 0$ and the angular distribution of the resonance structure in ejected electron spectra will be isotropic. Therefore any deviation from isotropy of the angular distribution of the resonance will provide strong evidence for the occurrence of angular momentum exchange during PCI.

3. Experimental details

The electron spectrometer used in the present work is similar to the apparatus described by Kuyatt and Simpson (1967). Electrons emitted by a tungsten filament are focused on the entrance of a hemispherical energy selector by cylindrical electrostatic lenses. After passing the energy selector the beam is directed into the interaction chamber containing helium gas at a pressure of 2×10^{-2} Torr. Scattered and ejected electrons leaving the interaction region at a variable angle θ are collected by a second system of electrostatic lenses and are energy analysed by a second hemispherical energy selector. The energy selectors are operated at a resolution of approximately 90 and 65 meV respectively.

Spectra are measured by counting and storing the number of pulses delivered by the electron multiplier in the subsequent channels of a multichannel analyser operating in the multichannel scaling mode synchronously with the sweep voltage. The sweep voltage is used to scan either the energy E_i of the incoming electrons or the energy E_c of the electrons transmitted by the analyser or E_i and E_c at the same time. In this way the electron spectrometer can be operated in three different modes.

(i) Constant ejected energy measurements. The transmission energy of the analyser is chosen such that ejected electrons from one or more autoionising states are detected: $E_c = E_{ej} = \text{constant}$, and the ejected electron yield is measured as a function of the

† Based on calculations of triple differential ionisation cross sections Tweed (1980, 1984) estimates by linear extrapolation to an electron energy of 0.5 eV, that the $l_i = 2$ partial wave at all angles contributes only to the fourth significant figure of the triple differential cross section.

incident energy. In the region $E_i > \text{IP} + E_{ej}$ (IP = 24.59 eV is the energy of the ground state of the He^+ ion) the ejected electrons are observed on an interfering background of electrons from the direct ionisation of helium. In the region $E_i < \text{IP} + E_c$ we observe a series of scattered electron peaks at positions $E_i = E^* + E_c$ corresponding to the singly excited states E^* of helium.

(ii) Constant incident energy measurements. In this mode we vary the transmission energy of the analyser to scan the region where ejected electrons from the autoionising states are observed. In the region $E_c = E_{ej} < E_i - \text{IP}$ PCI structures are observed on an interfering ionisation background. Below the ionisation threshold, in the region $E_c > E_i - \text{IP}$, peaks corresponding to the singly excited helium states are observed. In this region the post-collisional energy exchange between the ejected and the scattered electron is large enough for the latter to be captured into a singly excited state of the neutral atom.

(iii) Constant energy loss measurements: $E_l = \text{constant}$. We define the energy loss of the detected electrons as:

$$E_l = E_i - E_{ej}. \tag{3.1}$$

Depending on the value of E_l chosen two types of measurements are possible in this mode. We may measure the yield of scattered electrons from one of the singly excited helium states by chosing $E_l = E^* < \text{IP}$. We may also measure the yield of ejected electrons from the autoionising states by chosing $E_l > \text{IP}$, keeping the energy of the scattered electron (after autoionisation and PCI) constant: $E_i - E_{ej} = E_{sc} + \text{IP}$.

By measuring spectra in several modes of operation we may attain a view of how the different interference effects described in the previous sections manifest themselves.

Before and after each measurement the incident energy and energy loss scales are calibrated. The ejected electron energy then follows from equation (3.1). The energy loss scale is calibrated against the spectroscopically known positions of the helium singly excited states, whereas the incident energy scale is calibrated by fitting a Beutler-Fano profile to the $He^-(2s^22p)^2P$ and $He^-(2s2p^2)^2D$ resonances at 57.22 and 58.30 eV respectively. These resonance profiles are measured in the yield of scattered electrons from one of the $n = 2$ singly excited states of the helium atom, the spectrometer being operated in mode (iii).

In this calibration procedure we may account for instrumental broadening of the resonance profiles in the following manner. The cross section for an isolated resonance (energy E_r and width Γ) can be written down as follows (Feshbach 1962, Joachain 1975):

$$\sigma(E_i) = |T_{res}|^2 = \left| T_0 + \frac{a}{E_i - E_r + \frac{1}{2}i\Gamma} \right|^2 \tag{3.2}$$

where the complex amplitudes for direct and resonant scattering T_0 and a, respectively, only vary slowly with the incident energy E_i. It is convenient to rewrite this expression in the form (Shore 1967):

$$\sigma(E_i) = |T_0|^2 + \frac{A(E_i - E_r) + \frac{1}{2}B\Gamma}{(E_i - E_r)^2 + \frac{1}{4}\Gamma^2} \tag{3.3}$$

where $A = 2\,\text{Re}(T_0^* a)$ and $B = 2\,\text{Im}(T_0^* a) + 2|a|^2/\Gamma$. This formula is equivalent to the Beutler-Fano profile (see Comer and Read 1972). Convolution with a Gaussian profile

$$G(E) = \frac{1}{\sqrt{\pi} S} \exp(-E^2/S^2) \tag{3.4}$$

with FWHM $= 2S\sqrt{\ln 2}$ is easily performed using Abramowitz and Stegun (1964, equations (7.4.13) and (7.4.14)):

$$(\sigma * G)(E_i) = (T_0)^2 + \frac{\sqrt{\pi}A}{S} \operatorname{Im} W\left(\frac{E_i - E_r + \frac{1}{2}i\Gamma}{S}\right) + \frac{\sqrt{\pi}B}{S} \operatorname{Re} W\left(\frac{E_i - E_r + \frac{1}{2}i\Gamma}{S}\right). \tag{3.5}$$

This formula can be fitted to the spectra, using the numerical approximation by Gautschi (1969) (see also Kölbig 1972) of the complex error function:

$$W(z) = \exp(-z^2)\,\operatorname{erfc}(-iz). \tag{3.6}$$

In this way the resonance energies can be determined very accurately, thus providing a very accurate calibration of the incident energy scales of the ejected electron spectra. A typical inaccuracy of 10 mV is due to slight shifts of contact potentials during the measurements. Of course the absolute accuracy of the incident energy scale is determined by the accuracy with which the positions of the resonances are known.

4. Results

We have measured ejected electron spectra in all three modes described in the previous section and both interference effects discussed in § 2 appear to be present in the spectra. Figure 1 shows spectra measured at constant ejected electron energy. In the upper three spectra electrons ejected by the $He^{**}(2s^2)^1S$ autoionising state are observed. In the absence of post-collision interaction electrons ejected by this state have an energy of $E^{**} - \text{IP} = 33.23$ eV, so in the lowest spectrum we see electrons from the direct ionisation process only. No sloping background was subtracted from these spectra. The broad oscillations are due to the variation of the relative phase χ in equation (2.1) with incoming energy. Similar oscillations were observed by Baxter *et al* (1979) in the effective excitation functions of the $He^{**}(2s2p)^3P$ autoionising state. The rapid variations around $E_i = 58.30$ eV are caused by the presence of the $He^-(2s2p^2)^2D$ resonance. Note that structure due to decay of the resonance into the direct ionisation channel is very small or absent in the lowest spectrum so the variations around $E_i = 58.30$ eV in the upper three spectra are probably solely due to resonant excitation of the autoionising state. The size of the resonance appears to be strongly dependent on the ejected electron energy. We will comment on this further on.

Two other He^- resonances have been predicted theoretically (Nesbet 1976) in the energy region around 60 eV, namely the $He^-(2s2p^2)^2S$ state at 59.5 eV and the $He^-(2p^3)^2P$ state at 60.6 eV. They do not seem to affect the excitation cross section of the $He^{**}(2s^2)^1S$ state significantly, since no structure is observed at the appropriate energies in the spectra presented in figure 1.

In order to find evidence for possible angular momentum exchange during PCI we measured the angular distribution of the $He^-(2s2p^2)^2D$ resonance, observed in the ejected electron yield as a function of the incident energy. The results are presented in figure 2. The measurements were done at a constant ejected electron energy of $E_{ej} = 33.50$ eV, because the resonance is largest there as can be concluded from figure 3. The scattering angle was varied from 25° to 60°. Measurements at smaller angles are hampered by the very high direct ionisation background, whereas the mechanical construction of our electron spectrometer excludes measurements at larger angles. The range in which the incoming energy was varied was large enough to include observation of inelastically scattered electrons from the $n = 4$ singly excited states of helium, so

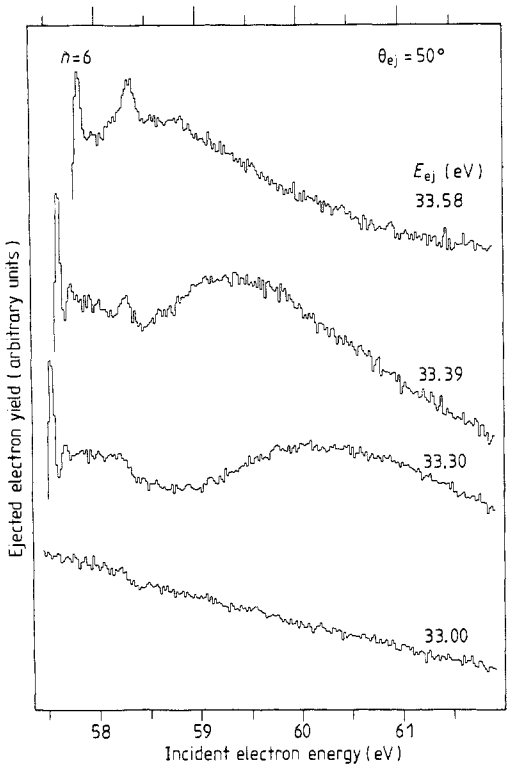

Figure 1. Ejected electron spectra measured with constant ejected electron energy at $\theta_{ej} = 50°$. The upper three spectra show electrons ejected by the $He^{**}(2s^2)^1S$ autoionising state, in the lowest spectrum only electrons due to the direct ionisation process are observed. All spectra were normalised on the direct ionisation cross section so that the vertical scales are comparable. The narrow peaks at the left show electrons having excited the $n = 6$ helium bound state.

that for each spectrum the ratio of resonance intensity to $n = 4$ singly excited state intensity could be determined. An additional series of spectra was measured at $E_{ej} = 33.50$ eV to determine the ratio of $n = 4$ to 2^1P singly excited state intensities. Thus a differential cross section for resonant excitation and decay of the $He^{**}(2s^2)^1S$ state (at a PCI energy exchange of 0.27 eV) could be obtained by multiplying the absolute differential cross section for the $1^1S \rightarrow 2^1P$ excitation at $E_i = 54.7$ eV by the product of the resonance to $n = 4$ intensity ratio and the $n = 4$ to 2^1P intensity ratio. Experimental 2^1P differential cross sections at $E_i = 55.5$ eV have been measured by Truhlar *et al* (1970), but we have used the tabulated values measured by Chutjian and Srivastava (1975) at 60 eV. Both measurements are in agreement with each other within the experimental error, which shows that the 2^1P differential cross section does not change very much around 55 eV. Therefore we do not introduce a large error by using the 2^1P differential cross sections at 60 eV. The error bars in figure 2(*a*) are mainly determined by the error in the resonance intensities, the error in the $n = 4$ to 2^1P intensity ratios being ±2%. The ±20% root mean square error in the 2^1P differential cross section quoted by Chutjian and Srivastava (1975) is not included in the error bars.

Figure 2(*a*) clearly shows that the angular distribution of the $He^-(2s2p^2)^2D$ resonance in the $He^{**}(2s^2)^1S$ ejected electron spectra is anisotropic. According to the

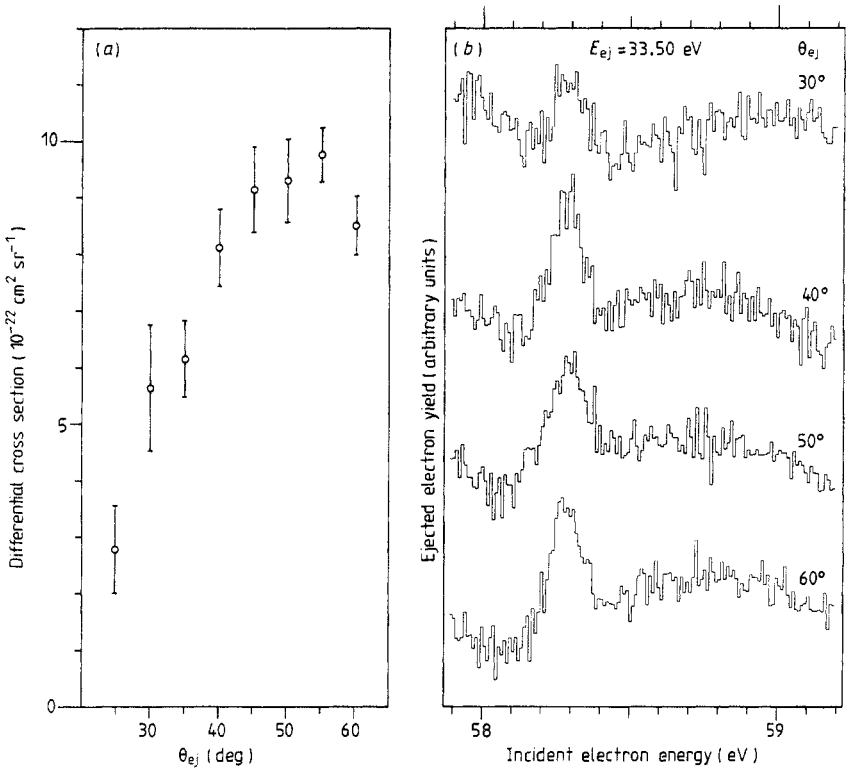

Figure 2. (*a*) Differential cross sections for resonant excitation and decay of the He**$(2s^2)^1$S autoionising state. The cross sections are determined for ejected electrons having acquired an extra energy of 0.27 eV during PCI. (*b*) Spectra measured with constant ejected electron energy at several angles. All spectra are normalised on the differential cross section for excitation of the helium 2^1P singly excited state. A linear sloping background was subtracted from the spectrum at $\theta_{ej} = 30°$.

discussion at the end of § 2 this shows that the electron ejected by the He**$(2s^2)^1$S autoionising state after resonant excitation must have exchanged orbital angular momentum with the scattered electron. The anisotropic angular distribution is the consequence of both angular momentum exchange during PCI and interference with electrons from the direct ionisation process. We conclude that a significant contribution to the size of the resonance comes from the interference term between autoionisation and direct ionisation. The very strong dependence of the size of the resonance on the energy the ejected electron acquires during PCI, as seen in figure 1, is a consequence of this interference. According to figure 2(*a*) we expect that the resonance disappears when an ejected electron spectrum is measured at $\theta_{ej} \simeq 20°$. This is in agreement with the results of van de Water and Heideman (1981). In their measurements at $\theta_{ej} = 22°$ a resonance effect is very small or absent.

Spectra measured at four different angles are shown in figure 2(*b*). As expected (see § 2.1) the shape of the resonance appears to be independent of the angle at which the ejected electrons are detected: at all angles it is a peak centred at $E_i = 58.30$ eV. Consequently the resonance to $n = 4$ intensity ratios mentioned above could be obtained easily by dividing the area under the resonance peak by the area under the peak of

scattered electrons from the $n = 4$ singly excited states. The symmetric resonance profiles in figure 2(b) suggest that direct excitation of the $He^{**}(2s^2)^1S$ state with the scattered electron receding in a $l_{sc} = 2$ wave is not very large at an incident energy of 58.30 eV. However, the peak positions in figure 2(b) lie approximately 20 meV below the resonance energy, indicating that there is some direct excitation of the autoionising state with the scattered electron receding in a $l_{sc} = 2$ wave.

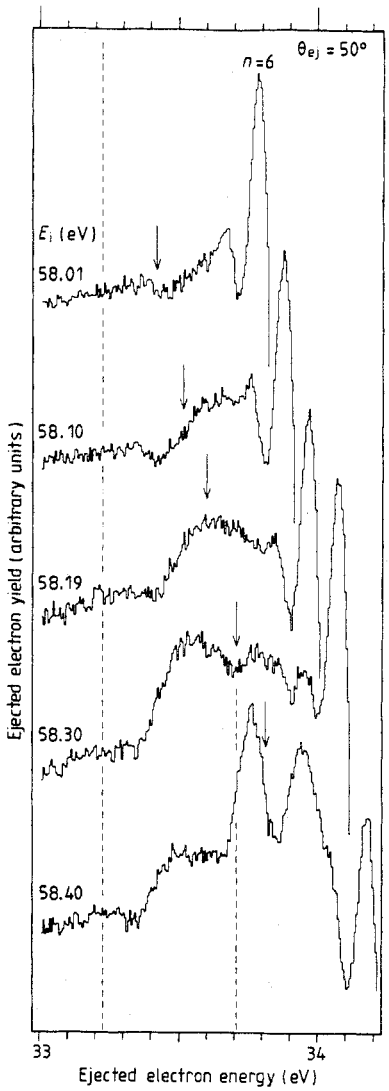

Figure 3. Ejected electron spectra measured with constant incident energy at $\theta_{ej} = 50°$. Vertical scales are comparable. The broken lines mark the nominal energies of ejected electrons from the $He^{**}(2s^2)^1S$ and $He^{**}(2s2p)^3P$ autoionising states; the ionisation threshold is indicated by the arrows. The large peak at the right in each spectrum is due to electrons having excited the $n = 6$ helium bound state.

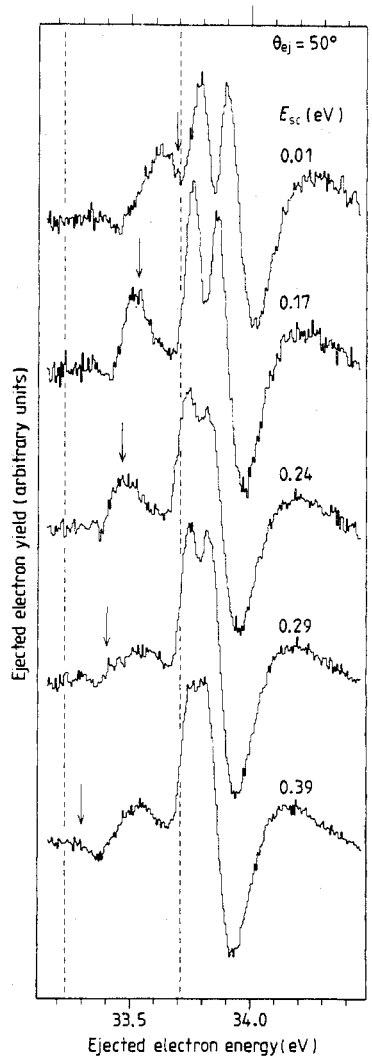

Figure 4. Ejected electron spectra measured with constant scattered electron energy at $\theta_{ej} = 50°$. In this mode the incident energy varies along with the ejected energy. Vertical scales are comparable. The broken lines mark the nominal energies of ejected electrons from the $He^{**}(2s^2)^1S$ and $He^{**}(2s2p)^3P$ autoionising states. The position of the $He^{-}(2s2p^2)^2D$ resonance on the incident energy scale is indicated by the arrows.

The total direct excitation of the $He^{**}(2s^2)^1S$ state (including all partial waves of the scattered electron) is already significant at 0.5 eV above its threshold. This result, which is contrary to the suggestion by Nesbet (1976), is clearly seen in figure 3. This figure shows ejected electron spectra measured in the constant incident energy mode. Between $E_{ej} = 33.23$ eV and $E_{ej} = 33.71$ eV, indicated by the vertical broken lines, we observe ejected electrons from the $He^{**}(2s^2)^1S$ state only. Above $E_{ej} = 33.71$ eV, but only in the lower two spectra, ejected electrons from the $He^{**}(2s2p)^3P$ autoionising state also contribute to the spectra. Below the ionisation threshold, at the right-hand side of the arrows, the scattered electron has lost so much energy during PCI that it is captured into a singly excited state of the helium atom. Between $E_{ej} = 33.23$ and 33.71 eV we see a significant PCI structure that gradually shifts to the right with decreasing incident electron energy. The larger PCI structure in the spectrum measured at $E_i = 58.30$ eV is due to an enhanced excitation cross section of the $He^{**}(2s^2)^1S$ state caused by the presence of the resonance. Contrary to the $He^{**}(2s^2)^1S$ autoionising state the threshold of the $He^{**}(2s2p)^3P$ state coincides with the position of the $He^-(2s2p^2)^2D$ resonance. The sharp rise in excitation cross section of this autoionising state, already reported by Spence (1975), is clearly seen in the lower two spectra in figure 3. Both broad peaks in the spectrum measured at $E_i = 58.40$ eV are due to ejected electrons from the $He^{**}(2s2p)^3P$ state interfering with electrons from the direct ionisation process. Part of the structure may be due to electrons ejected by the $He^{**}(2s^2)^1S$ state. A similar structure was measured by Baxter *et al* (1979) (see the lower spectra in their figure 1).

As described in § 3 ejected electron spectra may be measured in different modes of operation of the electron spectrometer. The spectra presented in the figures 1 and 3, which were measured with a constant ejected and incident energy respectively, in fact contain the same information. The spectra in figure 3 should be thought of as vertical sections through the spectra in figure 1. Consequently the spectra in figure 4, measured in the third mode of operation where both E_i and E_{ej} are scanned keeping the scattered electron energy constant, do not give new information, but this figure may serve as a consistency test of the measurements presented in the figures 1 and 3. Above $E_{ej} = 33.71$ eV marked by the right broken line we observe PCI profiles due to interference of ejected electrons from the $He^{**}(2s2p)^3P$ state with electrons from the direct ionisation process. Also ejected electrons from the $He^{**}(2s^2)^1S$ state may contribute to the observed structures. Between $E_{ej} = 33.23$ and 33.71 eV only electrons from the $He^{**}(2s^2)^1S$ state are present, interfering with a direct ionisation background. Figure 4 very clearly shows that the size of the resonance, whose position on the incident energy scale is marked by the arrows, depends strongly on the scattered electron energy. In the upper three spectra the resonance is very clearly visible whereas in the lower two spectra no resonant structure can be observed. This is in agreement with figure 1 which showed that the size of the resonance varies strongly with the ejected electron energy.

5. Conclusions

We have measured the angular distribution of electrons ejected by the $He^{**}(2s^2)^1S$ autoionising state after its excitation via the $He^-(2s2p^2)^2D$ resonance. Taking into account interference with electrons from the direct ionisation of helium, we were able to show that the observed anisotropic angular distribution is the result of an orbital angular momentum exchange during the post-collision interaction. This result casts

doubt on theoretical models for post-collision interaction which do not take into account angular momentum exchange at incident electron energies closer than 0.5 eV from threshold.

Contrary to previous suggestions near 58.3 eV only a part of the excitation of the $He^{**}(2s^2)^1S$ state is due to decay of the $He^-(2s2p^2)^2D$ resonance. Our measurements show that direct excitation of this autoionising state by electron impact is significant at incident electron energies of the order of 0.5 eV above its threshold.

Acknowledgments

This work was performed as a part of the research programme of the 'Stichting voor Fundamenteel Onderzoek der Materie' (FOM) with financial support from the 'Nederlandse Organisatie voor Zuiver Wetenschappelijk Onderzoek' (ZWO).

References

Abramowitz M and Stegun I A 1964 *Handbook of Mathematical Functions* (New York: Dover)
Baxter J A, Comer J, Hicks P J and McConkey J W 1979 *J. Phys. B: At. Mol. Phys.* **12** 2031-41
Chutjian A and Srivastava S K 1975 *J. Phys. B: At. Mol. Phys.* **14** 2360-8
Comer J and Read F H 1972 *J. Phys. E: Sci. Instrum.* **5** 211-2
Feshbach H 1962 *Ann. Phys., NY* **19** 287-313
Gautschi W 1969 *Commun. ACM* **12** 635
Heideman H G M 1980 *Coherence and Correlation in Atomic Collisions* ed H Kleinpoppen and J F Williams (New York: Plenum) pp 493-508
Hicks P J, Cvejanović S, Comer J, Read F H and Sharp J M 1974 *Vacuum* **24** 573-80
Joachain C J 1975 *Quantum Collision Theory* (Amsterdam: North-Holland)
Kölbig K S 1972 *Commun. ACM* **15** 465-6
Kuyatt C E and Simpson J A 1967 *Rev. Sci. Instrum.* **38** 103-11
Morgenstern R, Niehaus A and Thielmann U 1977 *J. Phys. B: At. Mol. Phys.* **10** 1039-58
Nesbet R K 1976 *Phys. Rev.* A **14** 1326-32
Niehaus A 1977 *Proc. 10th Int. Conf. on the Physics of Electronic and Atomic Collisions* ed G Watel (Amsterdam: North-Holland) Abstracts pp 185-200
Niehaus A and Zwakhals C J 1983 *J. Phys. B: At. Mol. Phys.* **16** L135-42
Read F H 1975 *Proc. 9th Int. Conf. on the Physics of Electronic and Atomic Collisions* ed J S Risley and R Geballe (Seattle: University of Washington) Abstracts pp 176-93
—— 1977 *J. Phys. B: At. Mol. Phys.* **10** L207-12
Shore B W 1967 *Rev. Mod. Phys.* **39** 439-62
Spence D 1975 *Phys. Rev.* A **12** 2353-60
Truhlar D G, Rice J K, Kupperman A, Trajmar S and Cartwright D C 1970 *Phys. Rev.* A **1** 778-802
Tweed R J 1980 *J. Phys. B: At. Mol. Phys.* **13** 4467-79
—— 1984 Private communication
van de Water W and Heideman H G M 1980 *J. Phys. B: At. Mol. Phys.* **13** 4663-74
—— 1981 *J. Phys. B: At. Mol. Phys.* **14** 1065-75
van de Water W, Heideman H G M and Nienhuis G 1981 *J. Phys. B: At. Mol. Phys.* **14** 2935-50